

Biodegradable mesh sheets as a treatment device for acute type A aortic dissection equipped with North American porcupine-inspired microneedle for removal prevention

Taiga Asami¹, Shunsuke Imamura¹, Tomoya Akaki¹, Kentaro Honda², Yoshiharu Nishimura², Atsushi Tanaka³, and Nobuhiro Kato^{4#}

¹ Graduate School of Biology-Oriented Science and Technology, Kindai University, 930 Nishimitani, Kinokawa, Wakayama, 649-6493 Japan
² Department of Thoracic and Cardiovascular Surgery, Wakayama Medical University, 811-1 Kimiidera, Wakayama, Wakayama, 641-8509 Japan
³ Department of Cardiovascular Medicine Wakayama Medical University, 811-1 Kimiidera, Wakayama, Wakayama, Japan
⁴ Faculty of Biology-Oriented Science and Technology, Kindai University, 930 Nishimitani, Kinokawa, Wakayama, 649-6493 Japan
Corresponding Author / Email: nkato@waka.kindai.ac.jp, TEL: +81-736-77-3888

KEYWORDS: Type A aortic dissection, Artificial tunica media, Biodegradable microneedle

A common repair for acute type A aortic dissection is anastomosis to replace the ascending aorta and hemi arc. Prior to the replacement, to obliterate the false lumen, the Bio glue is applied inside of the false lumen to reinforce the fragile nature of the disrupted aortic tissue. However, Bio glue has cytotoxicity which can damage fragile aortic tissue and cause re-dissection in long term due to its aldehyde compounds. On the other hand, microneedles have been researched for many decades as a transdermal drug delivery system. Dissolving or coated microneedle patches provide low-cost, rapid, pain-free, and direct way to deliver drugs into the dermal layer. From entirely different prospective, we previously reported that a biodegradable micro-needled mesh sheet (MNMS) to be a promising candidate of intracorporal topical hemostasis device that replace tissue-derived biomaterial to avoid a latently risk of infection. However, the MNMS, made with poly lactic acid (PLA), was required to improve its poor adhesion to soft tissue. Here we focused on North American porcupines' specialized barbs from a biomimetic point of view. The geometry of the barbs enables easy penetration and superior tissue adhesion. In this study, inspired by the barbs of North American porcupine, we developed a MNMS as an artificial tunica media made with biodegradable material to replace Bio glue in cardiovascular surgeries. The geometry of the supporting structure of the microneedles was designed to be compliant enough to fit soft tissue. The master mold of the MNMS was designed and modeled on a 3D CAD software (Fusion 360, Autodesk), and printed by an ultra-high resolution SLA 3D printer (SONIC MINI 8K, phrozen). A negative mold of the photocurable resin microstructure was obtained by silicone elastomer (Sylgard 184, Dow Corning) casting. A PLA mesh sheet with specialized mesh pattern was printed by using a FDM 3D printer (Pro2, RAISE). The final product, MNMS of PLA, was formed by heat imprinting of the PLA mesh sheet onto the elastomer female mold that has the microneedles and supporting structure relief pattern. Adhesive properties of MNMSs to Parafilm was examined by 90° peel test. As a result, the biomimetic geometry of the microneedle, inspired by the barbs of North American porcupine, improved the MNMS adhesion to parafilm up 70%. These findings should serve as the basis for the development of biodegradable MNMS to replace Bio glue in cardiovascular surgeries.

NOMENCLATURE

AAAD	=	acute type A aortic dissection
GRF	=	gelatin-resorcin-formalin
MN	=	microneedle
MNMS	=	microneedle mesh sheet
PLA	=	polylactic acid
SLA	=	stereolithography apparatus
CAD	=	computer-aided design
PDMS	=	polydimethylsiloxane
FDM	=	fused deposition modeling

1. Introduction

AADA is defined as a tear in the intima layer from the ascending aorta, which results in blood flow into the aorta media, forming true and false lumen. AADA is caused life-threatening complications (e.g., cardiac tamponade from hemopericardium, aortic regurgitation, stroke, aortic rupture, myocardial infarction). Without treatment, mortality rates are 1 to 2 percent per hour after symptom onset.¹⁾ A common repair for AAAD is anastomosis to replace the ascending aorta and hemi arc to artificial vessel. Prior to the replacement, applying GRF glue to obliterate the false lumen and reinforce the fragile nature. Bingley et. al. reported that the use of GRF glue develops postoperative midterm re-dissection due to the cytotoxicity of aldehyde compound.²⁾ As an alternative of GRF glue, fibrin glue has

been used for treatment of AAAD. However, the adhesive strength of fibrin glue, a biologically derived material, is obviously less than that of GRF glue. Hence, possibly cause re-dissociation. In recent years, Bio glue, have been employed in treatment for AAAD. The usage of Bio glue, however, has been concerned due to cytotoxicity which may cause postoperative midterm re-dissection and pseudoaneurysm formation.^{2,3)}

On the other hand, MNs have been studied as a drug delivery system for many decades. A MN patch provides a low-cost, rapid, pain-free, and direct way to deliver drugs into the dermal layer.⁴⁾ Yokoyama et. al. demonstrated a novel biodegradable MNMS as a promising candidate for treating intracorporeal topical hemostasis.⁵⁾ The MNMS was made of biodegradable thermoplastic produced from PLA.

In this study, we propose to apply a MNMS to be used as an *artificial tunica media* that reinforces disrupted fragile aortic tissue and enables the decrease of Bio glue usage. The drawback of the MNMS fabricated in previous studies is its poor adhesion to soft tissue. Here we focused on North American Porcupine's specialized barbs from biomimetic point of view.⁶⁾ The geometry of the barbs enables high penetration ability and adhesion ability. In this study, we introduce an ingenious MN design that inspired from North American Porcupine's barbs to adhere the soft tissue. To fabricate MNs with a complex structure, we developed a novel fabrication method of master mold of MNMS by using an ultra-high resolution SLA 3D printer. This method is rapid, cost effective, and simple. Adhesion property of the fabricated MNMS to parafilm was evaluated by 90° peel test.

2. Material and method

2.1 Fabrication of master mold of MN

First, we designed and modeled simple cone-shaped MN (870 μm in height, and 300 μm in base diameter) and 2 types of cone-shaped MN with simplified the North American Porcupine's barbs (6 and 8 barbs per a needle) on a 3D CAD software (Fusion 360, Autodesk). The master mold of MNs were printed by an ultra-high resolution SLA 3D printer (SONIC MINI 8K, Phrozen), with pixel size of $22 \times 22 \mu\text{m}^2$, and a step height of 5 μm using photo curable high-resolution resin (Aqua 8k Resin, Phrozen). The printed master mold was placed in isopropanol and cleaned in an ultrasonic cleaner (Hi-Power SUS-100, Shimadzu) for 2 minutes. After the sonication, the mold was spray rinsed with isopropanol and dried naturally for an hour in ambient atmosphere. Finally, the printed molds were cured in a cure system (UV-152, Ushio) for 110 minutes to eliminate PDMS curing inhibitors in the resin.⁷⁾

2.2 Fabrication of MNMSs

Female molds, the negative relief of the MNs, were obtained by PDMS (Sylgard 184, Dow Corning) pouring onto the master molds. The final product, MNMS made of PLA, was formed by heat imprinting process using a heater press (N4018-5K-200, NPA system) utilizing the female mold. Prior to the heat imprinting, a PLA mesh sheet was printed by using a FDM 3D printer (Pro2, RAISE). The geometry of the PLA mesh is shown in fig. 1. The mesh sheet of $100 \times 20 \text{ mm}^2$ with 1 mm^2 square unit cells was printed using a special G-code controlling the FDM 3D printer generated by original Python code. As shown in the Fig.2, the mesh sheet was placed between a

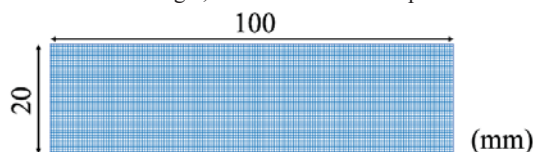


Fig. 1 Geometry of a PLA mesh.

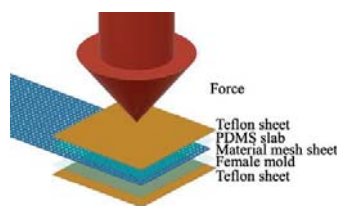


Fig. 2 Schematic of the heat imprinting

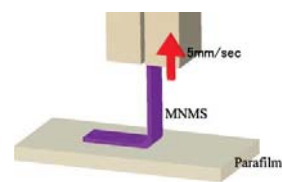


Fig. 3 Schematic of 90° peel test

PDMS slab and the female mold and heat imprinted to transfer the MN shape. The heat imprinted area was located 25 mm in width from the edge of the PLA mesh sheet. Conditions of the heat imprinting was 120°C, 50 seconds, and 800 N.

2.3 Adhesive quality characterization by 90° peel test

Adhesive quality of MNMS were evaluated based partially on a 90° peel test procedure (ISO29862:2007). As shown in the Fig.3, MNMS was peeled off from a situation of fully inserted into 7 layers of Parafilm (LABORATORY FILM, amcor), to the direction of perpendicular to the Parafilm surface by pulling for 30 mm at a speed of 5 mm/sec by a single axial tensile testing machine (EZ-SX, Shimadzu). The average value of the obtained force-displacement curve between 10 and 20 mm was used as the measurement value of MNMS adhesion force. Furthermore, the maximum pulling-off force was measured to determine the adhesive strength per one MN. The number of trials was 30 for each condition.

3. Result and Discussion

3.1 Fabrication of master mold of MN

SEM images of master mold of the simple cone-shaped MN, the master molds of the cone-shaped MN with 6 barbs and that of 8 barbs are shown in Fig.4 a, b and c, respectively. The length of MN was measured on the optical image obtained by a video microscope (SKL-Z300C, SAITOH KOUGAKU Co.Ltd). The length and the base diameter of simple cone-shaped MN were $602 \pm 4 \mu\text{m}$ and $309 \pm 9 \mu\text{m}$, respectively. Those of the cone-shaped MN with 6 barbs were $593 \pm 6 \mu\text{m}$, and $295 \pm 5 \mu\text{m}$, respectively. And those of the cone-shaped MN with 8 barbs were $635 \pm 16 \mu\text{m}$ and $307 \pm 6 \mu\text{m}$, respectively. Compared with the designed 3D model, the geometries of the printed MNs were increased by 27 ~ 32 % in height and decreased by 2 ~ 3 % in lateral direction. The increment of needle height originates from the so call layer shifting in the Z-axis of the 3D printer using the optical fabrication method. The decrement of the needle base diameter can be attributed to an anti-aliasing setup aiming to reduce the steps on the surface of the modeled object. Insufficiently exposed area on the periphery of the modeled object generated by the anti-aliasing was dissolved during the IPA rinse process.

3.2 Fabrication of MNMS

Thermally imprinted simple cone-shaped PLA MN, cone-shaped MN with 6 barbs and that of 8 barbs are shown in Fig.4 d, e and f, respectively. The length and the base diameter of simple cone-shaped MN were $564 \pm 19 \mu\text{m}$ and $323 \pm 13 \mu\text{m}$, respectively. Those of the cone-shaped MN with 6 barbs were $592 \pm 10 \mu\text{m}$ and $322 \pm 6 \mu\text{m}$, respectively. And those of the cone-shaped MN with 8 barbs were $597 \pm 12 \mu\text{m}$ and $323 \pm 13 \mu\text{m}$, respectively. Compared with the master mold, the geometries of the heat imprinted MNs were decreased by 0 ~ 6 % in height and increased by 5 ~ 9 % in lateral direction. These shape differences originate from the heat imprinting process with soft elastomer mold that deforms by the applied force during thermal imprinting process.

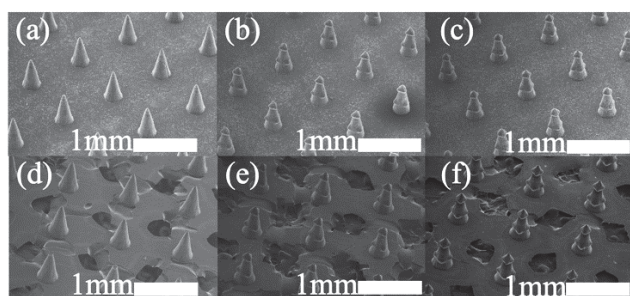


Fig. 4 SEM images of MNs. a) Master mold of simple cone-shaped MN. b) Master mold of MN with 6 barbs. c) Master mold of MN with 8 barbs. d) Replicated simple cone-shaped PLA MNMS. e) Replicated cone-shaped PLA MNMS with 6 barbs. f) Replicated cone-shaped PLA MNMS with 8 barbs.

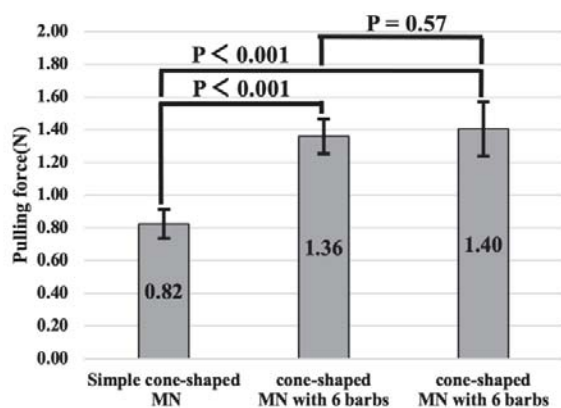


Fig. 5 The Averaged values of adhesive force in 10 mm ~ 20 mm peeling section. (n = 30)

Table 1 Comparison of the bioinspired barbed MNs

Reference	Length (μm)	Diameter (μm)	Max pull-out (mN/needle)	Material
[7]	4000	200	52 (muscle tissue)	Natural porcupine
[7]	5000	200	31 (porcine skin)	PU
[8]	2000	200	73 (rabbit skin)	CM-RF
[10]	1300	380	107 (parafilme)	Silk fibroin
cone shaped	564	327	62 (parafilme)	PLA
This work 6 barbs	597	323	93 (parafilme)	PLA
8 barbs	592	322	98 (parafilme)	PLA

3.3 Adhesive quality characterization by 90° peel test

Averaged values of adhesive force in a section between 10 mm and 20 mm are shown in Fig.5. Adhesive force of simple cone-shaped MN, cone-shaped MN with 6 barbs and that with 8 barbs were 0.82 ± 0.18 N, 1.36 ± 0.21 N and 1.40 ± 0.33 N, respectively. Compared with simple cone-shaped MN, the adhesive force of both cone-shaped MNs were increased in 70%. Adhesive strength tends to increase with the number of barbs. The MN adhesion was improved by the friction between the Parafilm and the MN due to barbs increasing the resistance to needle extraction.

Our MN achieved higher adhesive force compared to other reported state-of-the-art MNs (Table 1). Compared to the silk fibroin MN, the MN in this study had about the same adhesive strength even with less than half length. The MN length, diameter, and barbs can be controlled by modifying the 3D model, thereby controlling adhesion strength.

3. Conclusions

We developed novel master mold fabrication technique in MN production by using an ultra-high resolution SLA 3D printer. We mimicked and simplified the North American Porcupine's barbs and adopted in MN. As a result, the adhesion of MN with barbs was about 70% increased compared with simple cone-shaped MN. Furthermore, adhesive strength tends to be improved with the number of barbs. As a future task, the shape of apex of MN will be investigated to obtain easy penetration.

ACKNOWLEDGEMENT

This work was supported by KAKENHI (20K12658) .

REFERENCES

- Raimund, E., Victor, A., Catherine, B., Eduardo, B., Roberto, B., Holger, E., Arturo, E., Volkmar, F., Herbert, F., Oliver, G., Martin, G., Axel, H., Bernard, I., Athanasios, M., Folkert, M., Christoph, N., Marco, R., Herve, R., Udo, S., Per, S., Regula, and A., Christiaan, V., "2014 ESC Guidelines on the diagnosis and treatment of aortic diseases," *European Heart Journal*, 35, pp.2873–2926, 2014.
- John, B., Michael, G., E, S., Terrence, M., Peter, P., Robert, T., Homayoun, J., Peter, T., and Mark, O., "Late Complications of Tissue Glues in Aortic Surgery," *Ann Thorac Surg.*, 69, pp.1764-1768, 2000.
- Walter, F., MS., and Asmita, B., "Release of Glutaraldehyde From an Albumin-Glutaraldehyde Tissue Adhesive Causes Significant In Vitro and In Vivo Toxicity," *The Society of Thoracic Surgeons*, 79, pp.1522–9, 2005.
- "Medical Device Failure Report," Ministry of Health, Labour and Welfare., FY2021 Second Meeting of the Pharmaceutical Affairs and Food Sanitation Council, Subcommittee on Safety Measures for Medical Devices and Regenerative Medicine Products., 2-2-1, 2021.
- Yeu, K., Jung, P., and Mark, P., "Microneedles for drug and vaccine delivery," *Advanced Drug Delivery Reviews.*, 64, pp.1547-1568, 2012
- Mao, Y., Namie, C., Atsushim, T., Yosuke, K., Akira, T., Yuko, I., Mitsuru, Y., Kentaro, H., Yoshiharu, N., Toshikazu, K., Takashi, A., and Nobuhiro, K., "A biodegradable microneedle sheet for intracorporeal topical hemostasis," *Scientific Reports*, 10, pp.18831, 2020.
- Woo, C., James, A., Dagang, G., Shawn, C., Seung, Y., Anurag, K., Georgina, C., Robert, W., Ram, R., Rohit, K., Robert L, and Jeffrey, K., "Microstructured barbs on the North American porcupine quill enable easy tissue penetration and difficult removal," *PNAS*, Vol. 109 No. 52 pp.21289–21294, 2012.
- Bastien, V., Shanliang, D., Ziad, M., Aufried, L., Aurélie, C., Fabrice, B., Cees, O., Christian R., and Séverine, G., "PDMS Curing Inhibition on 3D-Printed Molds: Why? Also, How to Avoid It?," *analytical chemistry*, 93, pp.7180-7187, 2021.
- Zhipeng, C., Yinyan, L., Lei, R., Bin, L., Liang, L., Zhi, W., and Lelun, J., "Additive Manufacturing of Honeybee-Inspired Microneedle for Easy Skin Insertion and Difficult Removal," *ACS Appl. Master. Interfaces* 10, 29338, 2018.
- Le, T., Thanh, N., and Woo, P., "BIO-INSPIRED BAEDED MICRONEEDLE FOR SKIN ADHESION WITH INTERLOCKING MECHANICS," *MEMS2019*, pp.27-31, 2019.